ISSN 1330-3651 (Print), ISSN 1848-6339 (Online)
https://doi.org/10.17559/TV-20200419142656
Preliminary communication

Damage Deformation and Acoustic Emission Characteristics of Raw Coal under Different Moisture Contents

Huiqiang WU*, Fengyu REN, Dong XIA

Abstract: Coal seam with different moisture contents considerably affects coal mining and gas extraction. The coal seam with moisture contents has unique damage deformation characteristics that differ from dry coal. Therefore, the damage deformation characteristics of coal seam with different moisture contents need to be investigated to enhance the effects of coal mining and gas extraction. To explore the damage and deformation laws and acoustic emission (AE) characteristics of coal samples with different moisture contents, coal samples with different moisture contents were prepared for triaxial compression AE localization tests, and the stress-strain characteristic parameters and AE counts, cumulative AE counts, AE energy, and cumulative AE energy of coal samples were prepared. The damage models of coal samples with different moisture contents were established based on AE counts, and the damage and deformation laws were analyzed. Results show that the peak intensities of coal samples decrease with the increase in moisture contents, the dry coal sample mainly undergoes shear failure, and the water-containing coal samples are pronounced by lateral splitting. The peak and cumulative AE counts of the coal samples decreased as the moisture contents increased. The peak and cumulative AE energies of coal samples decreased with the increase in moisture contents. The damage model established based on AE counts has a high degree of fit. Moreover, the damage amount of the coal samples increased with the moisture contents. The conclusions obtained in this study have practical guiding significance for demonstrating the mechanism and process of coal body dynamic disasters in actual engineering.

Keywords: acoustic emission; characteristic parameter; coalmine safety; damage deformation; different moisture contents

1 INTRODUCTION

China's coal resources are abundant and high yielding. With the increase in mining depth and intensity, the engineering geological environment, in which raw coal masses are subjected to different changes, is also affected by groundwater at different levels. The differences in moisture content affect the mechanical properties of coal masses. In certain mining areas, the coal body is immersed for a long time, and the moisture content is increased because of the rising of the groundwater level, thereby reducing its bearing capacity, strength, and even damage [1]. Water exhibits physical effects (e.g., lubrication, softening, wet and dry, sludge, freezing, and thawing) on rocks [2]. During the excavation of underground engineering, the occurrence of disasters, such as rock bursts and coal and gas outbursts, is high, and water is an important factor that affects these disasters. Thus, domestic and foreign scholars have conducted considerable research on the water-rock interaction problem.

However, existing studies about coal with different moisture contents concentrate on a certain field, and a holistic research is severely lacking. Some academics study the uniaxial compressive strength of coal with different moisture contents, in stratum under the effect of tri-axial stress. In addition, the existing damage models of coal with different moisture content fitting degrees have poor quality.

In general, the stress-strain characteristic parameters of the coal samples are intimately connected with the acoustic emission (AE) characteristic parameters (e.g., AE counts, cumulative AE counts, AE energy, and cumulative AE energy). A damage model of coal with good fitting degree was built to analyze the relationship of the stress–strain and AE characteristic parameters of coal samples. This damage model fits the damage deformation law of coal with different moisture contents accurately. This study could provide a guiding function for coal mining and gas drainage.

2 STATE OF THE ART

Many scholars have conducted considerable research on water-rock interaction. Yao et al. [3] studied the strength, porosity, fracture propagation, and failure characteristics of coal with different moisture contents. The results show that the increase in moisture content promotes the change in the macroscopic failure mode of the coal samples from tensile failure to tensile-shear composite failure. Chen et al. [4] prepared and divided 54 coal–rock combinations equally into groups that contained different moisture contents to conduct AE testing under uniaxial compression with loading rates. The results show that the peak stress and strength-softening, elastic, strain-softening, and post-peak moduli partly decrease with the increase in moisture content and loading rate. Daraeiet al. [5] investigated an account of the effect of the water content on the critical and failure strains in considerable detail using uniaxial compression strength test results that pertained to 67 samples of 8 rock types under dry, natural, and saturated conditions. The results indicate that variations of the critical and failure strains have mainly occurred in water contents less than 2%. Zhao et al. [6] calculated the stresses at the tips of the compressive-sheared cracks by applying the superposition principle. The results show that the third principal stress of the main crack surface significantly increases the rock strength when the internal friction angle of the rock is lower than the crack inclination angle. Wang et al. [7] explored the influence of temperature and time on water-rock interactions and conducted saturation experiments on ore rock and gneiss samples under different temperatures and soaking times. The results show that temperature changes the intensity of the water-rock interactions. Qian et al. [8] performed uniaxial compressive tests on coal specimens with different water-soaking heights to gain an improved understanding of different water-soaking height-induced weakening characteristics of coal. The results show that the AE activities of complete water-soaking and non-soaking coal specimens are relatively concentrated, occurring

mainly in the unstable fracture expansion and post-peak destruction stages, and AE exhibits a main-shock mode. Bian et al. [9] investigated the mechanism of parameter degradation for shale under immersed conditions from the microscopic perspective with the aid of X-ray diffraction and scanning electron microscopy. He established a damage constitutive model of rock subjected to the water-weakening effect and uniaxial loading by considering the influence of the void-compression stage. Guoet al. [10] tested the uniaxial cyclic loading to study the mechanical behaviour of dry and water-saturated igneous rock with AE monitoring. The results suggest that the groundwater can reduce the burst proneness of igneous rock but increase the potential support failure of the surrounding rock in the igneous-invaded area. Hashibaet al. [11] investigated the effects of water saturation on the loading rate dependence of strength, which was a time-dependent characteristic of rocks, theoretically and experimentally. The test results show that rock strength increases with the decrease in water saturation, and an increment in strength accompanied by a tenfold rise in loading rate is almost constant under various water saturation conditions. Heggheim et al. [12] analyzed the softening of sandstone and examined the main factors that affected water–rock interaction, including sandstone particle changes, cement composition, pore morphology, and pore size. Sun et al. [13] emphasized that the increase in moisture content would weaken rock strength and reduce the cumulative AE counts and cumulative energy during rockburst. Tutuncuet al. [14] experimented the Berea sandstone immersed in different saturated solutions under the cyclic uniaxial stress condition and discussed the attenuation mechanism of the hysteresis loop in the deposited granular rock. Burshtein [15] studied the effects of moisture contents on the uniaxial compressive strength of rocks. Ahamedet al. [16] introduced a method to change the mechanical properties of coal based on coal-water interaction. Lu et al. [17] studied the water absorption experiments of dehydrated coal. Wang et al. [18] explored the effects of moisture on coal permeability. Pereraet al. [19] compared the strength and deformation characteristics of saturated and dry coal samples. Pan et al. [20] conducted loading and unloading tests on coal bodies under five states of moisture contents and analyzed the relationships between the moisture contents and the elastic modulus of coal. Qin et al. [21] measured the AE characteristics of the entire uniaxial compression of square coal samples with different moisture contents and compared the stress-strain characteristics and damage evolution laws of coal samples with different moisture contents during uniaxial compression. Shao et al. [22] studied the mechanical properties of sandstone under different water conditions. Jing et al. [23], Wei et al. [24], and Jiang et al. [25] analyzed the influences of moisture contents on the characteristics, mechanical properties, and energy dissipation of coal permeability. Wu et al. [26] analyzed the characteristics of overlying strata fracture and law of evolution of separation fissures under hard and thick strata in underground coal mining and further revealed the occurrence of dynamic disasters. Abadieet al. [27] reviewed PHES and its ability to support intermittent generation from energy plants, such as wind and solar, thereby preventing energy losses and storing energy for use at times of high demand. Yin et al. [28] developed two experimental equipment of gas-containing coal under static and dynamic loading to investigate the static and dynamic mechanical properties of coal under various gas pressures. Zhang et al. [29] proposed a multisource information integration model of geographic information system after using the analytic hierarchy process to determine the weights of indicators, thereby establishing an integrated prediction model and studying the regularity of water abundance.

Most of the extant studies have focused on the mechanical characteristics of non-coal rock masses under different moisture contents, whereas few studies have been conducted on raw coal masses. Therefore, in this study, triaxial compression AE localization tests were conducted on raw coal under different moisture contents. The damage deformation and AE characteristics of raw coal with different moisture contents (e.g., 0%, 0.5%, and 1.5%) were investigated, and damage models were established. AE is an important precursor to the instability of rock compression fractures. Studying the characteristics of AE of rock compression fractures and the use of AE monitoring technology to prevent dynamic disasters, such as rockburst and coal and gas outbursts, can provide a deep understanding of rock failure mechanisms. Disasters have important theoretical and practical significance [30]. The results of this study potentially provide a design basis for future gas drainage and outburst prevention measures [31]. They also have practical significance for the engineering design of raw coal masses with different water-bearing states during mining.

The remainder of this study is organized as follows. Section 3 describes the specimen preparation and testing program. Standard coal with different moisture contents has been prepared and tested with triaxial compression, and the AE characteristic parameter has been recorded by using an acoustic emission imaging acquisition instrument. Section 4 provides the interpretation of results and analyzes the stress–strain and AE characteristic parameters to build the damage model with evolutionary analysis. Section 5 summarizes this study and provides the results.

Figure 1 Raw coal samples

3 METHODOLOGY

3.1 Preparation of Samples

The coal samples were selected from the Jishan Mining Chengshan Coal Mine. The coal samples were processed into standard coal samples with a height of 100

mm and a diameter of 50 mm according to the requirements of the regulations. To reduce the influence of coal sample body moisture on the test, four coal samples were dried before the test, the temperature was set to 60 °C, and the coal samples were weighed with a balance with an accuracy of 0.01 g. After drying, the coal samples were immersed in water at different times, and the coal samples were weighed again after being immersed in water. Water immersion tests were performed to prepare samples with 0%, 0.5%, and 1.5% moisture contents (Fig. 1). The detailed parameters of the coal sample are shown in Tab. 1.

Table 1 Parameters of coal samples

Number	Quality / g		Moisture content	Diameter / mm	Height / mm	Cell pressure / MPa	Peak intensity / MPa	Residual intensity / MPa
	Before immersion	After immersion						
S1	270.77	270.77	0%	50.57	101.43	15	35.94	28.31
S2	293.85	295.30	0.5%	50.53	101.67		31.80	29.73
S3	268.82	272.91	1.5%	50.40	101.53		24.88	23.85

3.2 Experimental Plans

RTX-1000 high-temperature and high-pressure dynamic rock triaxial instrument (Fig. 2) and a Micro-II high-temperature and high-pressure AE imaging acquisition instrument were used in this study. Six AE sensors were installed on the coal sample (Fig. 3). The numbers on the figure represent the positions where the sensors are installed. AE characteristic parameters are synchronized by an AE imaging acquisition instrument. A strain sensor is installed on the rock triaxial apparatus to synchronize the mechanical characteristics of the coal samples in the triaxial compression test. To ensure the detection effects of the AE signals during the deformation and failure of the samples, the heat shrink tube is closely adhered to the surface of the coal sample to prevent the penetration of silicone oil from causing damage to the coal sample. The AE instrument has six channels, and the threshold value is set to approximately 45 dB. The threshold value is continuously adjusted to a maximum of 70 dB using the sound test of pencil lead breaking.

Figure 2 RTX-1000 high temperature and high pressure dynamic rock triaxial instrument

The test was first loaded to a predetermined confining pressure of 15 MPa, and the coal samples with different moisture contents (e.g., 0%, 0.5%, and 1.5%) were compressed at a strain rate of 0.005%/min until failure. The mechanical characteristics and acoustic parameters of the entire process were analyzed. Correspondence between emission characteristic parameters was developed, damage models were established, and the damage deformation processes were analyzed.

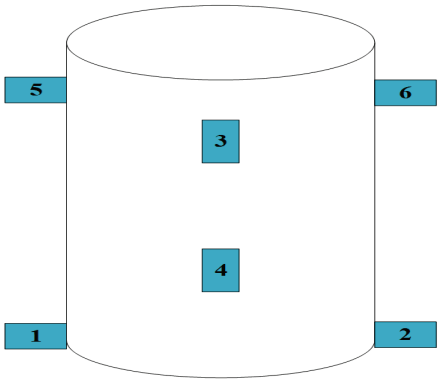

Figure 3 Acoustic emission sensors layout

4 RESUILT ANALYSIS AND DISCUSSION

4.1 Analysis of Stress-Strain Characteristics

The full stress–strain curves of coal samples with different moisture contents were obtained through tests (Fig. 4). According to Fig. 4, the compacted coal sample in the dry state has consumed shorter time and has a longer elastic deformation phase. The deformation before reaching the peak intensity shows almost a linear deformation trend. After the peak intensity was reached, stress decreased rapidly, and the coal sample deformed greatly. With the increase in moisture content, the compaction phase time of coal samples is long, and the elastic phase time is short. Shortly after compression, the stress–strain curves began to bend and did not show a linear deformation trend. The peak intensity of the dry coal sample is 35.94 MPa, and the residual intensity is 28.31 MPa. The peak intensity of 0.5% moisture content coal sample is 31.80 MPa, and the residual intensity is 29.73 MPa. The peak intensity of 1.5% moisture content coal sample is 24.88 MPa, and the residual intensity is 23.85 MPa. With the increase in moisture content, the peak intensities of coal samples gradually decrease, and the residual intensities also show a decreasing trend because of the softening effect of water on coal samples. On the one hand, water weakens the cohesive force between particles inside the coal sample; on the other hand, it expands the pore fissures between particles within the coal sample, thereby extending the microfissures through. As the rate increases, the intensities of the coal samples decrease. During compression failure, the brittle deformation of the dried coal sample is significant. With the increase in

moisture contents, the plastic and coal sample deformations are evident.

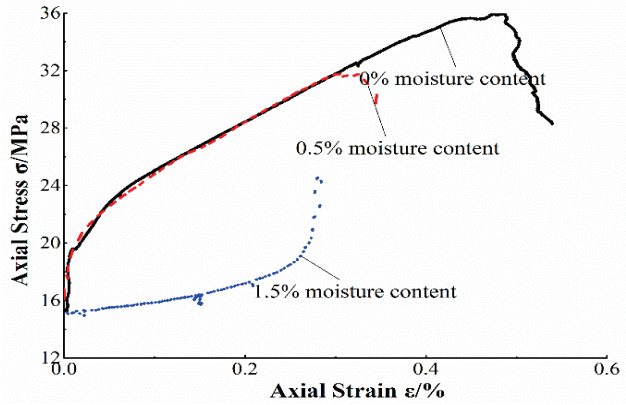

Figure 4 Stress and strain process curves

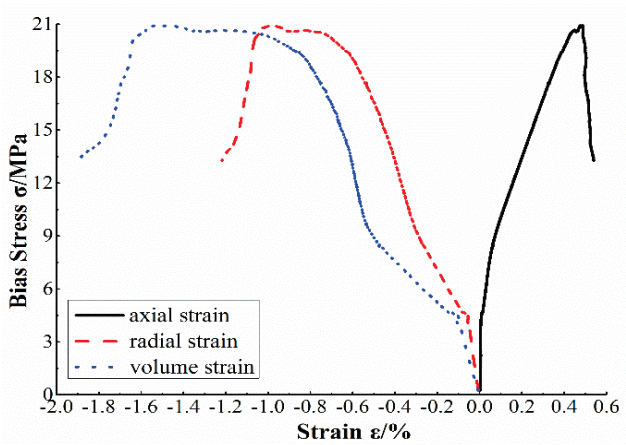

(a) Coal sample with 0% moisture content

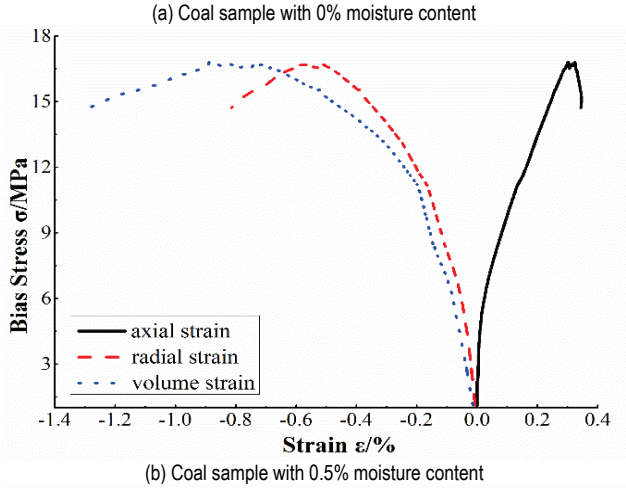

(b) Coal sample with 0.5% moisture content

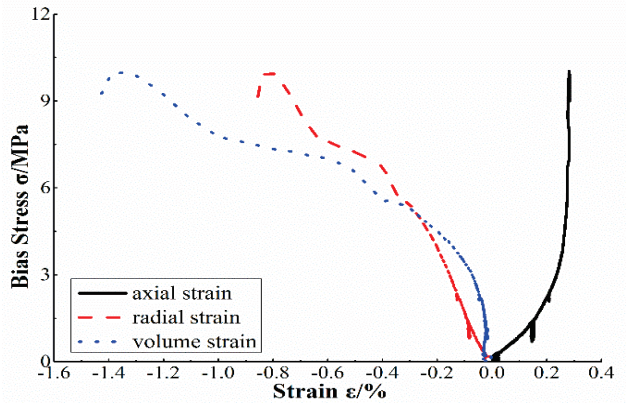

(c) Coal sample with 1.5% moisture content

Figure 5 Stress and strain curves

The deformation characteristics of the coal samples are analyzed according to the stress-strain curves of the coal samples with different moisture contents (Fig. 5) combined with the state of the damaged coal samples (Fig. 6).

The curves in Fig. 5 indicate that the stress–strain curves of the coal samples with different moisture contents show the same law. The radial strain rates of the coal samples are greater than the axial strain rates, negative volume strains occur, and the coal samples indicate dilatation and expansion. In the elastic phase, the volumes show a linear decreasing trend, and then the curves turn and begin to expand. As the strain increases, the curves change nonlinearly, but the volumes of the coal samples are almost unchanged. Subsequently, the volume strain curves increase with the strains. The volumes of the coal samples rise, and the coal samples expand laterally, thereby reaching the expansion stage.

In combination with the coal samples states in Fig. 6, the dry coal sample undergoes shear failure, and the crack on the surface of the coal sample exhibits a certain angle with the axial loading direction. As the moisture content increased, the position of the microcracks gradually expanded to the middle of the coal sample, and a macrocrack parallel to the centerline of the coal sample was generated because the coal samples in the test absorbed water but did not fully reflect the lubricating effect of water, causing the internal cracks of the coal sample to build up damage and form large cracks at the position of the coal sample loading centerline gradually.

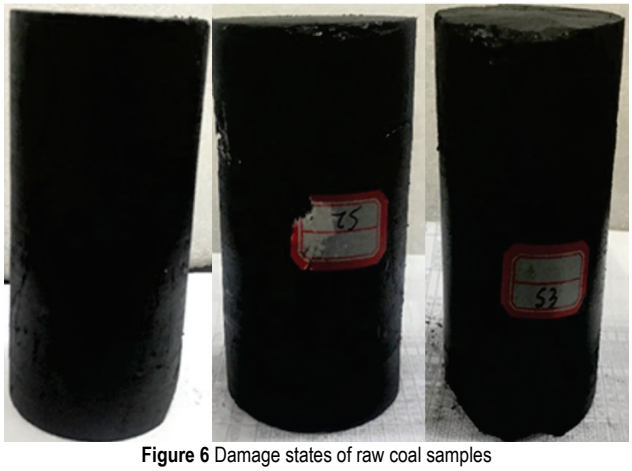

Figure 6 Damage states of raw coal samples

4.2 Analysis of AE Characteristic Parameters

The analyses of stress and strain parameters of coal samples obtained from triaxial compression tests with AE characteristics parameters and drawing stress–strain count curves and cumulative count curves of coal samples with different moisture contents (Fig. 7) and stress–strain energy curves and cumulative energy curves (Fig. 8) were combined. The curves of Fig. 7 and Fig. 8 indicate that the AE count and AE energy change trends of coal samples with different moisture contents are similar to the stress–strain curves change laws.

With the increase in the moisture content, the water molecules weaken the cohesion between the particles, the softening of the water prevents the internal cracks from expanding through the coal sample, and the AE signal declines. Therefore, the higher the moisture content, the

lower the peak AE counts, and the more the cumulative AE counts low. The peak AE count of the dry coal sample is 690 times, and the cumulative AE count is 105,161 times. The peak AE count of 0.5% moisture content coal sample is 546 times, and the cumulative AE count is 29 400 times. The peak AE count of 1.5% moisture content coal sample is 249 times, and the cumulative AE count is 23 938 times. Under the action of water, the intensity of the coal sample, the external load required to achieve destruction, and the energy released are reduced. Therefore, the higher the moisture content, the lower the peak AE energy, and the lower the cumulative AE energy. The peak AE energy of the dry coal sample is 672 J, and the cumulative AE energy is 39 154 J. The peak AE energy of the 0.5% moisture content coal sample is 474 J, and the cumulative AE energy is 18 892 J. The peak AE energy of the 1.5% moisture content coal sample is 380 J, and the cumulative AE energy is 16 742 J.

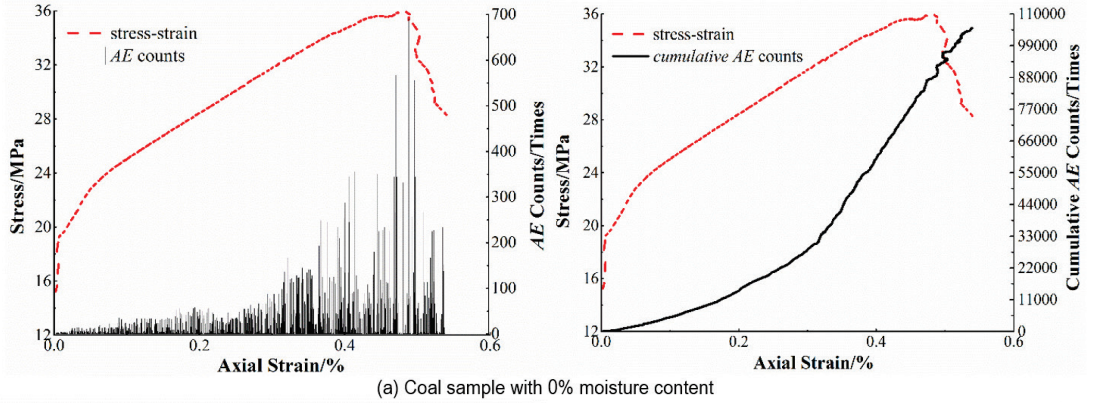

(a) Coal sample with 0% moisture content

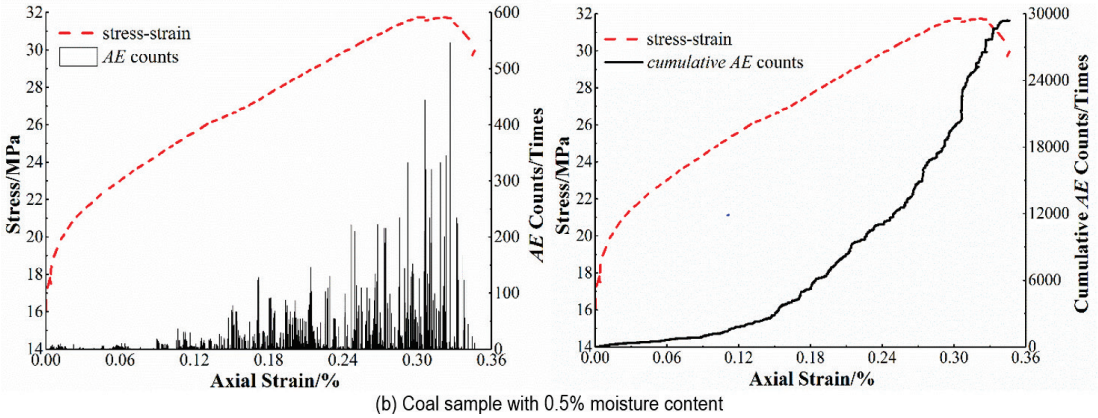

(b) Coal sample with 0.5% moisture content

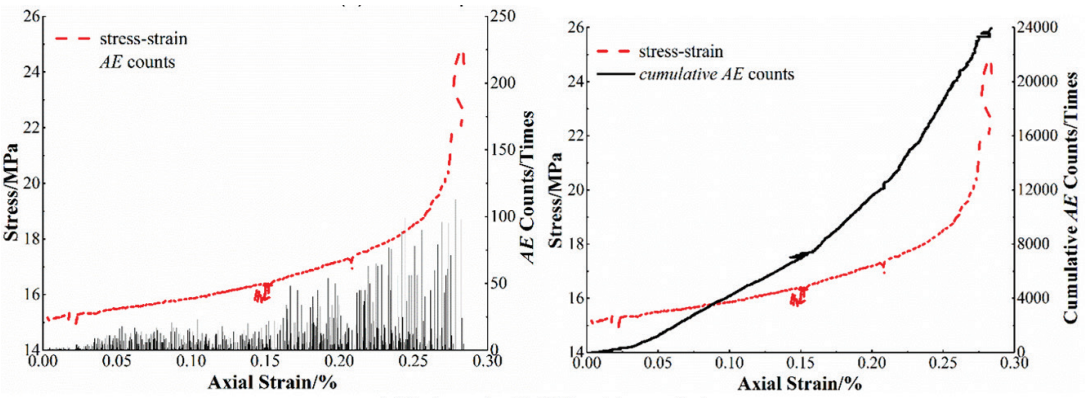

(c) Coal sample with 1.5% moisture content

Figure 7 Stress-strain counts and cumulative counts curves of coal samples under different moisture contents

(1) In the stage of crack compaction, the time for drying coal samples is relatively short. Given that the original cracks are compacted and closed, unrecoverable residual deformation occurs, and few AE signals appear. Then, the AE counts and AE energy are small, and the stress–strain curves appear as a concave. The fracture compaction stage of coal samples with 0.5% moisture content and 1.5% moisture content is relatively long. Shortly after compression, the nonlinear bending of the stress-strain curves appeared. Owing to the softening effect of water, the compaction closure of the internal fractures of the coal samples is destroyed, thereby reducing the number of AE signals, AE counts, and AE energy.

(2) In the elastic phase, the AE signal is relatively stable, the time for drying the coal sample is longer, and the stress–strain curves show linear elastic growth. With the increase in moisture content, the AE signals of coal samples in the elastic stage are less than those of the dry coal sample, and the AE counts and AE energy are lower.

As the moisture contents increase, the AE counts and AE energy decrease.

(3) During the elastoplastic stage, additional cracks are generated in the dry coal sample to expand and penetrate, the AE signals increase rapidly, the AE counts and AE energy increase sharply, and the stress-strain curves show nonlinear growth. The increase in the moisture contents hinders the crack propagation and penetration because of the softening effect of water; the AE counts and AE energy are much smaller than that of the dry coal sample; and the AE counts and AE energy decrease with the increase in the moisture content.

(4) In the failure stage, the AE signals are the strongest, the AE counts and AE energy reach the peak, and the internal cracks in the coal samples form macrocracks, which are unstable and damaged.

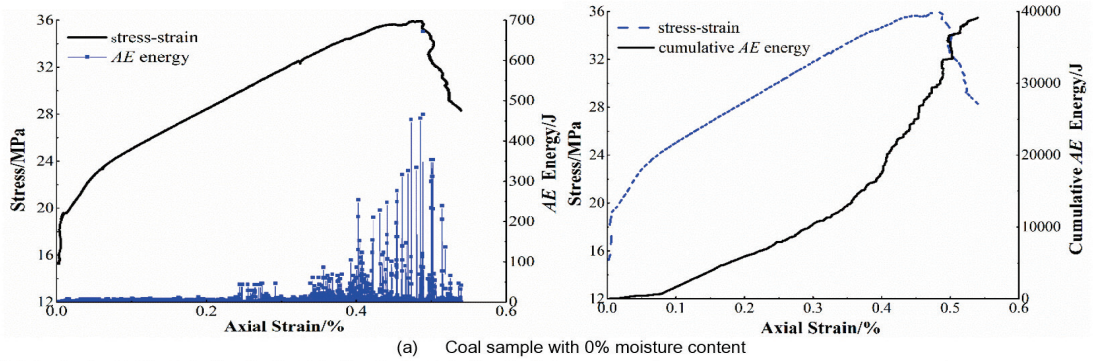

(a) Coal sample with 0% moisture content

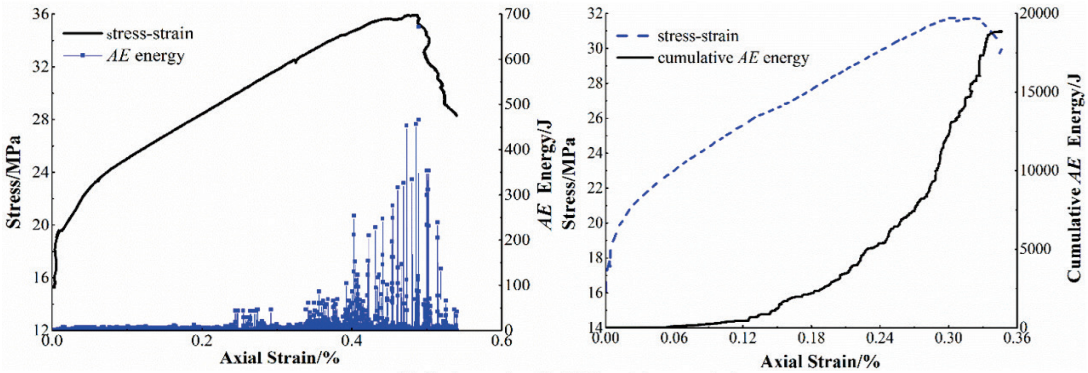

(b) Coal sample with 0.5% moisture content

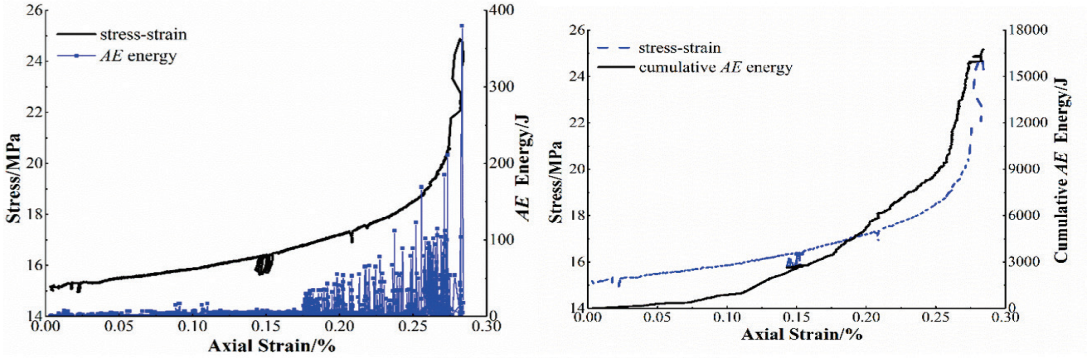

(c) Coal sample with 1.5% moisture content

Figure 8 Stress-strain energy and cumulative energy curves of coal samples under different moisture contents

4.3 Damage Evolution of Coal Samples with Different Moisture Contents

4.3.1 Establishment of a Damage Model

Damage refers to the phenomenon that the material's microdefects under load cause the viscous cohesive force to weaken progressively and even undergo micro-element failure. Its related theory has been the focus of rock mechanics research [32]. According to Kachanov's damage theory, the damage variable is defined as [30]

$$D = \frac{A_d}{A} \tag{1}$$

where D is the damage variable of the coal sample; A_d is the total area of the micro-defects on the load section, mm^2; and A is the cross-section area without damage, mm^2.

The AE count C_w when the micro-element per unit area is destroyed is

$$C_w = \frac{C_0}{A} \tag{2}$$

where C_w is the AE count when the micro-element per unit area is broken, times; and C_0 is the cumulative AE count of the complete damage of the non-destructive material, times.

When the cross-section damage area reaches A_d, the cumulative AE count C_d is:

$$C_d = C_w A_d = \frac{C_0}{A} A_d \tag{3}$$

where C_d is the cumulative AE count when the cross-section damage area reaches A_d, times; and C_w is the AE count of the micro area damage per unit area, times.

Thus,

$$D = \frac{C_d}{C_0} \tag{4}$$

Where D is the damage variable of the coal sample.

$$D = D_U \frac{C_d}{C_0} \tag{5}$$

where D_U is the damage threshold.

C_0 is the cumulative AE count when the damage variable reaches D_U. For simplicity of calculation, the damage threshold is taken as:

$$D_U = \frac{\sigma_C}{\sigma_P} \tag{6}$$

where σ_P is the peak intensity, and σ_C is the residual intensity.

The damage variables were calculated on the basis of the above formula, and the damage test curves were drawn. The origin selection function was used to fit the nonlinear curve, damage theory curve was drawn, and the damage law and the fitting degree of the two curves were analyzed. The ExpDec1 exponential function was selected as the fitting function because the damage test curve of the coal samples conformed to the exponential function growth law; that is, the damage of coal samples was relatively mild in the early stage and exponential in the later stage.

The coal-damage theory curve equation is:

$$D = D_0 \tag{7}$$

where D_0 is the initial damage value of the coal sample; ε is the strain, %; and M and n are constants.

The detailed parameters are shown in Tab. 2.

Table 2 Parameters of the theoretical curve equation

Moisture contents, %	D_0	M	n	Fit
0	−0.04	0.03	−0.24	0.99
0.5	−0.01	0.01	−0.09	0.99
1.5	−0.07	0.06	−0.12	0.99

4.3.2 Analysis of Damage Evolution

The experimental and theoretical curves of the coal damage model are shown in Fig. 9. Based on the curve evolution rule, the damage curves can be divided into four stages, namely, the initial damage, the stable damage development, the accelerated damage development, and the damage destruction stages. We combined the damage stages with the AE stages of coal samples, and the analysis is presented as follows.

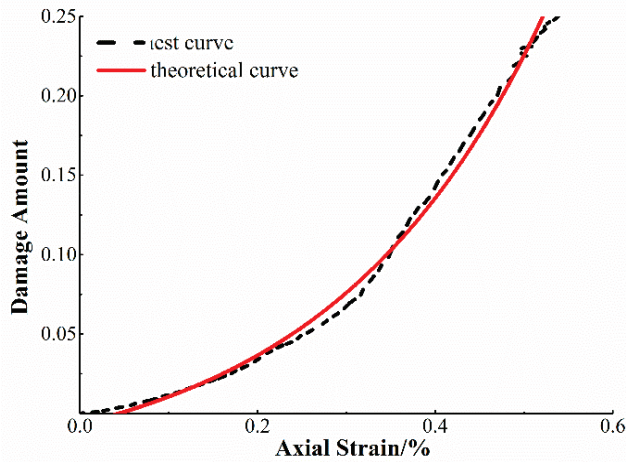

(a) Coal sample with 0% moisture content

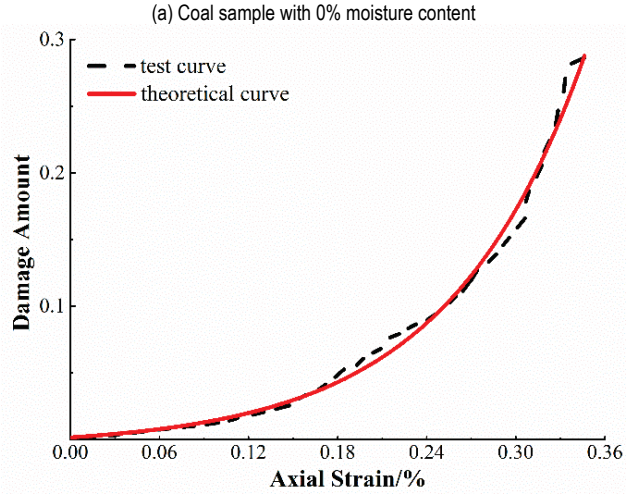

(b) Coal sample with 0.5% moisture content

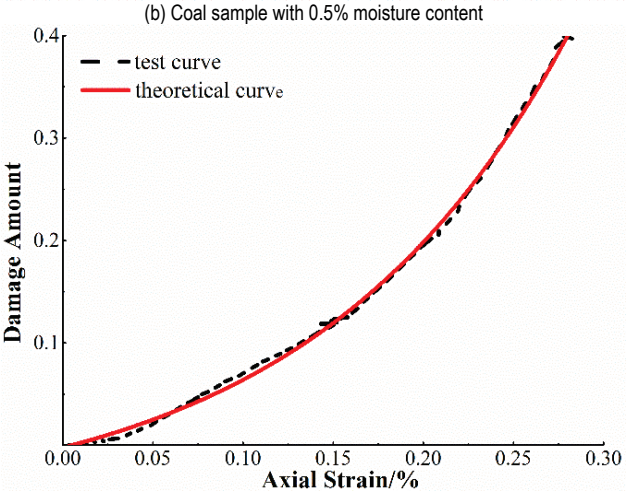

(c) Coal sample with 1.5% moisture content

Figure 9 Experimental and theoretical relationship curves of coal samples damage with different moisture contents

(1) Initial damage stage: the cracks inside the coal samples are compacted and closed during the compaction phase, and almost no new cracks are generated during the elastic deformation phase. AE signals, AE counts, and AE energy are low, and the corresponding coal sample damage approaches 0.

(2) Stable development stage of damage: the deformation of the coal samples enters the elastoplastic deformation stage; more cracks are generated and

expanded inside the coal sample, the AE signals increase rapidly, the AE counts and AE energy increase sharply, and the amounts of damage at this time continuously increase.

(3) Accelerated damage development phase: severe AE signals are generated, the AE counts and AE energy continue to increase and reach a peak, the cracks inside the coal samples expand and form macro-cracks, and the corresponding damage amounts continue to increase steadily.

(4) Damage and damage stage: After the macrodamage of coal samples, a certain carrying capacity remains, and the AE signals rapidly decrease and stabilize at a certain value. At this time, the damage amounts gradually stabilize.

Additional cracks spread through the dried coal sample, the AE signal is strong, and the AE count and AE energy are high. The increase in the moisture contents hinder crack propagation and penetration because of the softening effect of water. The AE signals are weaker, and the AE counts and AE energy are much smaller than those of the dry coal sample. The damage of dry coal samples is 0.25, the damage of 0.5% moisture content in the coal sample is 0.30, and the damage of 1.5% moisture in the content coal sample is 0.40. With the increase in moisture content, the damage of coal samples increases because the effect of water weakens the intensities of the coal samples and decreases the stress intensities of the coal samples. Therefore, under the condition of applying the same load, the higher the moisture content, the greater the damage of the coal samples. The fitting degrees of the coal sample curves in Tab. 2 indicate that the curve equation can simulate the damage strain curve of the coal sample remarkably. The fitting degree of coal samples with different moisture contents is 0.99, which is close to 1, thereby representing a higher degree.

However, the establishment of the model did not analyze the damage evolution law of coal samples comprehensively. The damage of coal samples is discrete, and the local damage is not considered for safety. This situation needs to be continuously improved in future research.

Fig. 10 reports the comparison of the corresponding damage–strain curves of coal samples with different moisture contents. It shows that the damage amount of dry coal sample is 0.25, the damage amount of coal sample with 0.5% moisture content is 0.30, and the damage amount of coal sample with 1.5% moisture content is 0.40. The amount of damage in the coal samples increases with the moisture contents. The axial strain when the dry coal sample is broken is 0.54, the axial strain when the 0.5% moisture content coal sample is broken is 0.34, and the axial strain when the 1.5% moisture content coal sample is broken is 0.28. The deformation of the coal samples is small as the moisture contents increase mainly because of the softening of water, which reduces the intensities of coal samples and the release of energy when coal samples are damaged under the same load conditions. The plastic deformation of coal samples increases with the moisture contents. Coal fractures are caused by the accumulation and penetration of microcracks, whereas the brittleness of the dried coal sample is high, and large-scale fractures are formed by macrocracks during failure.

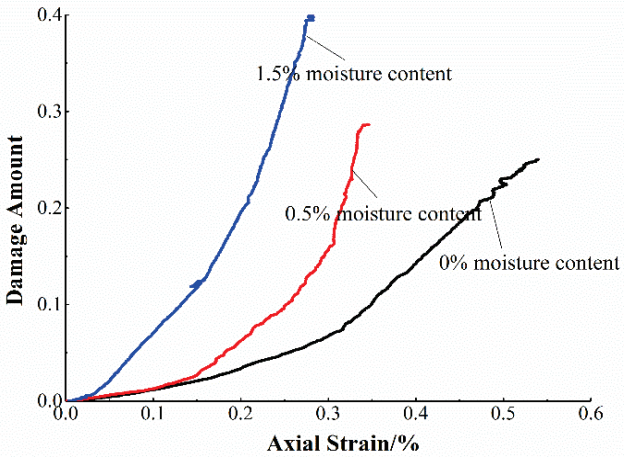

Figure 10 Corresponding curves of damage strain of coal samples with different moisture contents

5 CONCLUSION

This study tested the coal samples with different moisture contents, analyzed the stress–strain characteristic parameters and AE counts, cumulative AE counts, AE energy, and cumulative AE energy of coal samples; and built the damage model of coal samples with different moisture contents via the triaxial compression AE experiment. The conclusions of this study are detailed as follows.

(1) The softening effect of water reduces the peak and residual intensities of coal samples with the increase in moisture content.

(2) The radial strain rates of the coal samples become greater than the axial strain rates as the strain increases. Negative volume strains occur, and the coal samples undergo dilatation and deformation. Shear failure is the main factor that causes the failure of the dry coal sample. As the moisture contents increase, the lateral splitting failures of water-containing coal samples occur.

(3) With the increase in the moisture contents, the internal cracks of the coal samples are blocked from expanding and penetrating, the AE counts and AE energy decrease, and the cumulative AE counts and energy decrease. Moreover, the AE counts and the AE energy of water-containing coal samples are smaller than those of the dry coal sample.

(4) Damage and deformation models for coal samples with different moisture contents are established on the basis of AE counts. As the moisture content increases, the amounts of damage in the coal samples increase, and the curve fitting degrees approach 1. The model fits the coal samples well in different conditions. The damage evolution process continues depending on the water content, but it still needs to be improved in future research.

The results of this study are preliminary and are based on the coal samples with different moisture contents. These results are determined by triaxial compression acoustic emission experiment, analysis of the stress–strain characteristic parameters and AE counts, cumulative AE counts, AE and cumulative AE energy, the damage model and deformation characteristic and with different moisture content. Questions, such as the damage model and deformation characteristic of other moisture contents and

coal-rock sample sizes, need to be investigated in the future.

Acknowledgements

The study was jointly supported by grants from the Key Program of National Natural Science Foundation of China (Grant no. 51534003) and National Key Research and Development Program of China (Grant no. 2016YFC0801601).

6 REFERENCES

[1] Xiao, H., Yang, Z. Y.,Cui, Q. L., et al. (2014). Effect of standing water in closed pit mine goaf on the stability of waterproof coal pillar. *Coal Science and Technology,* (4), 105-107.

[2] Li, T. B., Chen, Z. Q., Chen, G. Q., et al. (2015).Research on energy mechanism of sandstone under different moisture content. *Rock and Soil Mechanics,* (s2), 229-236.

[3] Yao, Q. L., Zheng, C. K., Tang, C. J., et al. (2020). Experimental investigation of the mechanical failure behavior of coal specimens with water intrusion. *Frontiers in Earth Science*, 7, 348. https://doi.org/10.3389/feart.2019.00348

[4] Chen, T., Yao, Q. L., Wei, F., et al. (2017). Effects of water intrusion and loading rate on mechanical properties of and crack propagation in coal–rock combinations. *Journal of Central South University, 24*(2), 423-431. https://doi.org/ 10.1007/s11771-017-3444-6

[5] Daraei, A. & Zare, S. (2018). Effect of water content variations on critical and failure strains of rock. *KSCE Journal of Civil Engineering, 22*(9), 3331-3339. https://doi.org/10.1007/s12205-018-0592-7

[6] Zhao, Y. L., Wang, Y. X., Tang, L. M., et al. (2019). The compressive-shear fracture strength of rock containing water based on druker-prager failure criterion. *Arabian Journal of Geosciences, 2*(15), 452-460. https://doi.org/10.1007/s12517-019-4628-1

[7] Wang, F., Cao, P., Cao, R. H., et al. (2019). The influence of temperature and time on water-rock interactions based on the morphology of rock joint surfaces. *Bulletin of Engineering Geology and the Environment, 78*(5), 3385-3394. https://doi.org/10.1007/s10064-018-1315-5

[8] Qian, R. P., Feng, G. R., Guo, J., et al. (2019). Effects of water-soaking height on the deformation and failure of coal in uniaxial compression. *Applied Sciences-Base, 9*(20), 4370. https://doi.org/10.3390/app9204370

[9] Bian, K., Liu, J., Zhang, W., et al. (2019). Mechanical behavior and damage constitutive model of rock subjected to water-weakening effect and uniaxial loading. *Rock Mechanics and Rock Engineering, 52*(1), 97-106. https://doi.org/ 10.1007/s00603-018-1580-4

[10] Guo, J., Feng, G. R., Qi, T. Y., et al. (2018). Dynamic mechanical behavior of dry and water saturated igneous rock with acoustic emission monitoring. *Shock and Vibration*, 2348394. https://doi.org/10.1155/2018/2348394

[11] Hashiba, K., Fukui, K., & Kataoka, M. (2019). Effects of water saturation on the strength and loading-rate dependence of andesite. *International Journal of Rock Mechanics and Mining Sciences,* 117, 142-149. https://doi.org/10.1016/j.ijrmms.2019.03.023

[12] Heggheim, T., Madland, M. V., Risnes, R.., et al. (2014). A chemical induced enhanced weakening of chalk by seawater. *Journal of Petroleum Science and Engineering, 46*(3), 171-184. https://doi.org/10.1016/j.petrol.2004.12.001

[13] Sun, X. M., Xu, H. C., Zheng, L. G., et al. (2016). An experimental investigation on acoustic emission characteristics of sandstone rockburst with different moisture contents. *Science China Technological Sciences, 59*(10), 1549-1558. https://doi.org/10.1007/s11431-016-0181-8

[14] Tutuncu, A. N., Podio, A. L., & Sharma, M. M. (1998). Nonlinear viscoelastic behavior of sedimentary rocks, part ii: hysteresis effects and influence of type of fluid on elastic moduli. *Geophysics, 63*(1), 195-203 https://doi.org/10.1190/1.1444313.

[15] Burshtein, L. S. (1969). Effect of moisture on the strength and deformability of sandstone. *Soviet Mining, 5*(5), 573-576. https://doi.org/10.1007/BF02501278

[16] Ahamed, M. A. A., Peera, M. S. A., Matthal, S. K., et al. (2019). Coal composition and structural variation with rank and its influence on the coal-moisture interactions under coal seam temperature conditions: A review article. *Journal of Petroleum Science and Engineering,* 180, 901-917. https://doi.org/10.1016/j.petrol.2019.06.007

[17] Lu, X. F., Liao, J. J., Mo, Q., et al. (2019). Evolution of pore structure during pressurized dewatering and effects on Moisture readsorption of lignite. *ACS Omega,* 4(4), 7113-7121. https://doi.org/10.1021/acsomega.9b00381

[18] Wang, S. G., Elsworth, D., & Liu, J. S. (2013). Permeability evolution during progressive deformation of intact coal and implications for instability in underground coal seams. *International Journal of Rock Mechanics & Mining Sciences,* 58, 34-45. https://doi.org/10.1016/j.ijrmms.2012.09.005

[19] Perera, M. S. A., Ranjith, P. G., & Peter, M., (2010). Effects of saturation medium and pressure on strength parameters of Latrobe Valley brown coal: Carbon dioxide, water and nitrogen saturations.*Energy,36*(12), 6941-6947. https://doi.org/10.1016/j.energy.2011.09.026

[20] Pan, Z., Connwll, L. D., Camilleri, M., et al. (2010). Effects of matrix moisture on gas diffusion and flow in coal. *Fuel, 89*(11), 3207-3217. https://doi.org/10.1016/j.fuel.2010.05.038.

[21] Qin, H., Huang, G., & Wang, W. Z. (2012). Experimental study on acoustic emission characteristics of compressive deformation and failure of coal rocks with different moisture content. *Chinese Journal of Rock Mechanics and Engineering, 31*(6), 1115-1120.

[22] Shao, M. S., Li, L., Li, Z. X., et al. (2010). Elastic wave velocity and mechanical properties of longyou grotto sandstone under different water conditions. *Chinese Journal of Rock Mechanics and Engineering, 29*(S2), 3514-3518.

[23] Jing, J. J., Liang, W. G., Zhang, B. N., et al. (2016). Experimental study on the influence of water content on gas seepage characteristics of coal seams. *Journal of Taiyuan University of Technology, 47*(4), 450-454.

[24] Wei, J. P., Qin, H. J., Wang, D. K., et al. (2014). Study on seepage characteristics of gas-containing coal under loading-unloading confining pressure based on water effect .*Journal of Mining and Safety Engineering, 31*(6), 987-994.

[25] Jiang, C. B., Duan, M. K., Yin, G. Z., et al. (2016). Experimental study on loading and unloading of gas-containing raw coal under different water-containing conditions. *Journal of China Coal Society, 41*(09), 2230-2237.

[26] Wu, Q. S., Jiang, L. S., Wu, Q. L., et al. (2018). A study on the law of overlying strata migration and separation space evolution under hard and thick strata in underground coal mining by similar simulation. *Dyna, 93*(2), 175-181. https://doi.org/10.6036/8678

[27] Abadie, L. M. & Goicoechea, N. (2019). Review and analysis of energy storage systems by hydro-pumping to support a mix of electricity generation with a high percentage of renewables. *Dyna, 94*(6), 669-675. https://doi.org/10.6036/9182

[28] Yin, Z. Q., Zhang, Z., Ma, H. F., et al. (2018). Experimental study on the static and dynamic mechanical properties of

coal under different gas pressures. *Journal of Engineering Science and Technology Review, 11*(4), 61-68. https://doi.org/ 10.25103/jestr.114.08

[29] Zhang, H. M., Wu, J. W., Wang, G. T., et al. (2018). Combination of GIS and AHP methods to predict water abundance of sandstone aquifer in coal seam roof. *Journal of Engineering Science and Technology Review, 11*(2), 48-53. https://doi.org/10.25103/jestr.112.08

[30] Duan, M. K., Jiang, C. B., Gan, Q., et al. (2019). Experimental investigation on the permeability, acoustic emission and energy dissipation of coal under tiered cyclic unloading. *Journal of Natural Gas Science and Engineering*, 73, 103054. https://doi.org/10. 1016/j.jngse.2019.103054.

[31] Zhang, M. B., Lin, M. Q., Zhu, H. Q., et al. (2018). An experimental study of the damage characteristics of gas-containing coal under the conditions of different loading and unloading rates. *Journal of Loss Prevention in the Process Industries, 55*, 338-346. https://doi.org/10.1016/j.jlp.2018.07.006.

[32] Niu, Q. H. (2017). *Experimental study on shear failure damage of water-containing coal samples,* M. A. Thesis. Xuzhou: China University of Mining and Technology.

[33] Wang, D. C. (2011). *Acoustic Emission Mutation and Prediction of Rock Triaxial Compression Fracture Instability*, M. A. Thesis. Shandong: Shandong University of Science and Technology.

Contact information:

Huiqiang WU, PhD, Lecturer,
(Corresponding author)
School of Resources and Civil Engineering,
Northeastern University,
Shenyang, Liaoning, China
E-mail: qianghuiwu@163.com

Fengyu REN, PhD, Professor,
School of Resources and Civil Engineering,
Northeastern University,
Shenyang, Liaoning, China
E-mail: happyrst@163.com

Dong XIA, PhD, Lecturer,
College of Mining and Engineering,
North China University of Science and Technology,
Tangshan, China
E-mail: dianjiahan@163.com